Physica Scripta. Vol. 52, 506–510, 1995

Lifetime measurements in N III using the beam-foil technique and cascade corrections

P. Bengtsson, L. J. Curtis, M. Henderson, R. E. Irving and S. T. Maniak

Department of Physics and Astronomy, University of Toledo, Toledo, Ohio 43606, U.S.A.

Received February 19, 1995, accepted in revised form May 19, 1995

Abstract

Lifetime measurements are reported for several levels in the 2s2p3p, 2s2p3d, $2s2p^2$, $2p^3$ configurations of boronlike N III. Beam-foil excitation methods were used with cascade repopulation analyzed by the correlated decay curve ANDC technique. A small but significant J-dependence in the lifetimes of the $3d\,^4F$ levels was observed. The experimental lifetimes for the levels in the $2s2p^2$ and $2p^3$ were found to be in good agreement with recent theoretical results.

1. Introduction

Experimental studies of the lifetime differences among the individual fine structure levels within a term system can provide a sensitive test of atomic structure calculations. Even for term systems that are in other ways accurately described by *LS* coupling, very small changes in the wave function composition can produce substantial J-dependent lifetime variations by, *e.g.*, opening additional decay channels. Such a J-dependence in the measured lifetimes of the $2s2p3p\,^4D$ and $2s2p3d\,^4F$ levels in boronlike F V was reported [1] in 1991. In the same year, similar lifetime measurements of the isoelectronic counterparts of these levels in N III were also reported [2], but for that case no significant J-dependent variations were found. This isoelectronic discrepancy led to the experimental investigation of the lifetimes of these levels in O IV [3] (the intervening member of this sequence), where J-dependent variations were also observed. Calculations of these lifetimes for N III–F V have been reported [4] using the technique of Cowan [5] for fitting of the Slater parameters to the observed energy levels. An *ab initio* calculation of these transition rates using MCHF methods has also been reported for C II–F V [6]. These calculations agree with the experimental measurements for O IV and F V, and also predict a small but significant difference in the lifetimes for the fine structure components of the $3p\,^4D$ and $3d\,^4F$ levels in N III. We have undertaken a reinvestigation of these lifetimes in N III, with special care given to the effects of cascade repopulation and line blending.

Lifetimes can be extracted from decay curve measurements either by multiexponential fitting of individual decay curves, or by joint analysis of cascade-correlated decay curves by the ANDC method [7, 8]. For this system, the measurements for O IV [3] and F V [1] employed both of these methods, and obtained mutual consistency. In the N III measurement [2], cascade-corrected lifetimes for the $3p\,^4D$ level were reported, but the $n = 4$ complex was not included in the analysis. Cascade-corrected lifetime measurements for the fine structure levels of the $2s2p3p\,^4P$ term have been performed [9] and other lifetime measurements of various quartet levels in N III have been reported [10–15].

Line blending also affects the analysis of N III. As the nuclear charge Z decreases along an isoelectronic sequence, the wavelength separation between the lines in a multiplet decreases and the wavelengths become longer. Thus, both the resolution of the lines in a multiplet and the ion-beam energy needed to produce these states decrease with decreasing Z. The lower ion-beam energy introduces a larger Doppler broadening of the lines, and the longer wavelengths require the use of gratings with lower dispersion, both further limiting the resolution. In addition, the longer wavelengths can require the use of detectors with higher background noise. Thus, in the F V study [1], all of the fine structure components in $3d\,^4F$ and $3p\,^4D$ could be measured, but in the O IV study [3], it was not possible to experimentally resolve transitions from the $^4F_{3/2}$ and $^4F_{5/2}$ levels, and the $3p\,^4P_{1/2}$–$3d\,^4D_{1/2}$ line was impossible to resolve from a blend.

We have also investigated the decay rates of $2s2p^2$ and $2p^3$ levels in N III, which are of recent interest as a result of their application to the determination of the abundance of nitrogen in stars and in the interstellar medium [17–19]. Brage *et al.* [19] have recently reported extensive calculations in N III, which motivates our measurement of the lifetimes of the $2s2p^2$ doublet and the $2p^3\,^4S_{3/2}$ levels and those that cascade into them. The $2s2p^2\,^4P$ levels in N III are inaccessible to beam foil measurement because of their long lifetimes, but they have been measured by Fang *et al.* [18] using ion trap methods. Reistad *et al.* [20] have studied the $2s2p^2$ doublets in the isoelectronic system C II, and there extensive cascade analysis was found to be necessary. In this investigation we have also measured as many as possible of the N III $2s2p^2$ doublet and $2p^3\,^4S_{3/2}$ transitions and their cascades.

2. Experiment

The measurements were performed utilizing the 30–330 kV Danfysik Heavy Ion Accelerator at the University of Toledo [21] to produce an isotopically pure beam incident on an exciter foil. The energy of the ions in a typical run was 250 keV, which is lower than the optimum energy for the production of N^{2+}, but provided greater machine stability. The emitted radiation was analysed using an Acton 1 m normal incidence VUV monochromator, using three different sets of gratings and detectors. A 600 l/mm grating blazed at 3000 Å was used in combination with a photomultiplier tube to measure the (2s2p core) $3p\,^4D$–$3d\,^4F$, the $3s\,^4P$–$3p\,^4D$, the $3s\,^4P$–$3p\,^4P$ and the $3s\,^4P$–$3p\,^4S$ lines. A

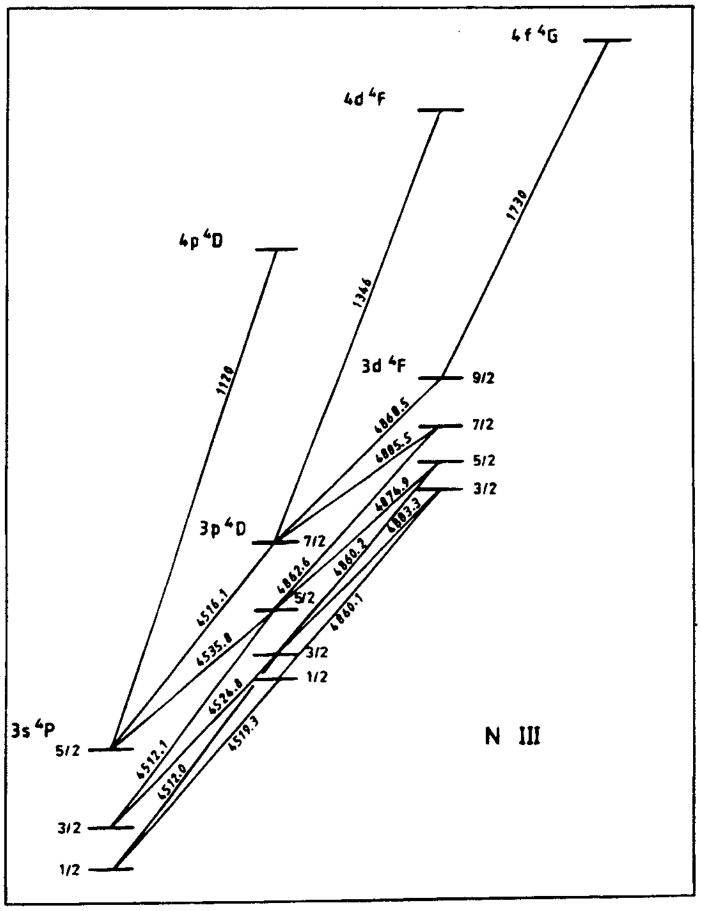

Fig. 1. Level diagram of selected terms in the 2s2p*nl* quartet system with wavelengths for the transitions.

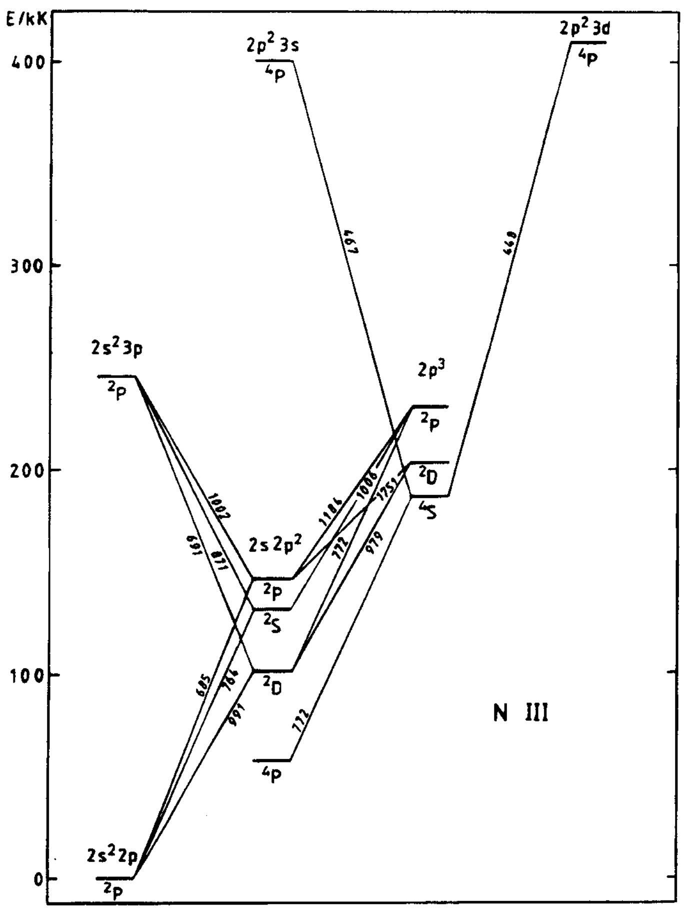

Fig. 2. Level diagram of the terms in the $2s2p^2$ and $2p^3$ configurations and the levels cascading into them.

1200 l/mm grating blazed at 1500 Å was used with a solar blind detector to measure the 3p ^{4}D–4d ^{4}F and 3d ^{4}F–4f ^{4}G lines. Finally, a 2400 l/mm grating blazed at 800 Å was used with a channeltron detector to measure lines in the range 400–1200 Å. The experiment was computer controlled by an on-line data acquisition system [22].

The targets were self-supporting carbon foils, with thicknesses kept low at 2.1–2.4 μg/cm^2 to minimize post-foil beam divergence. The pressure in the target chamber was maintained below 10^{-6} torr to achieve negligible collisional deexcitation. The beam current was typically kept at 250 nA to optimize the usable life of the foils, so as to permit the decay curves of the long-lived 3p ^{4}D and 3d ^{4}F levels to be measured over the full 120 mm length of the chamber. The foil-induced beam divergence for these thin foils is estimated to be sufficiently small to ensure that the entire beam profile is contained within the monochromator viewing volume over the full foil travel. Two methods for normalizing the intensity were available: current normalization using a Faraday cup; and light normalization using an optical fibre that views the beam at a fixed distance slightly downstream from the foil. The optical normalization was found to be more reliable for these long decays (at the extreme upstream position of the foil, the divergence of the beam can cause incomplete collection in the Faraday cup), and was used in the analysis of the data. The current normalization was also monitored as a sensitive measure of possible foil degradation and the formation of pinholes, and provided criteria for rejection of imperfect data sets.

Decay curves were obtained by stepwise translation of the foil upstream relative to monochromator slit. All decay curves were recorded starting with the foil positioned slightly downstream of the monochromator slit, so that the position of the foil could be accurately located on each of the measured decay curves. This provides the common zero point of excitation time for the cascade-correlated decay curves that is necessary for the ANDC analysis [8]. The foils were stepped upstream until the tail of the decay curve signal was small relative to the background.

The energy levels of N III are known from the analysis of Michels [23], and a tabulation of the lines is available in Ref. [24]. As was the case in the O IV analysis [3], it was not possible to measure transitions from all fine structure levels in the 3p ^{4}D and 3d ^{4}F terms because of blends within the multiplet or with transitions in other charge states. The level system with the wavelengths for the transitions of interest for the discussion here is shown in Fig. 1. The 3d $^4F_{5/2}$ and 3d $^4F_{3/2}$ decay curves could not be separately measured, but were investigated as an admixture in the blend of the 3p $^4D_{1/2}$–3d $^4F_{3/2}$ and 3p $^4D_{3/2}$–3d $^4F_{5/2}$ transitions that occurs at 4860 Å. Unfortunately, the 3p $^4D_{5/2}$–3d $^4F_{5/2}$ line at 4874.96 Å, which could provide a means to deconvolute this blend, was too weak to be measured. The 3p $^4D_{1/2}$ level was not accessible to measurement because the 3s $^4P_{1/2}$–3p $^4D_{1/2}$ transition was too weak. The analysis of 3p $^4D_{5/2}$–3d $^4F_{7/2}$ and 3p $^4D_{3/2}$–3d $^4F_{5/2}$ is complicated by a blend with a N II line at 4861.53 Å (3p $^3D_1$–3d $^1D_2$). However, the decay curve of 3d $^1D_2$ can be measured in another channel and a judgement of the importance of that blend can be made. In contrast to the 3d ^{4}F levels in F V and O IV where the inclusion of the cascade from the 4f ^{4}G level was sufficient for correlated decay curve analysis, in N III it was necessary to include cascades from both the 4f ^{4}G and 4p ^{4}D levels in the analyses. The decay curve of the 4p ^{4}D was measured via the branch to 3s ^{4}P, and, as in the case of the 3p ^{4}D–4d ^{4}F and 3d ^{4}F–f ^{4}G transitions, it was measured in an unresolved multiplet. The same is true for the cascade to 2p^3 $^4S_{3/2}$, which was measured in two unresolved multiplets at 467 Å for the 2p^{2}3s ^{4}P term and at 448 Å for the 2p^{2}3d ^{4}P term. Here we refer to Fig. 2.

3. Analysis

All decay data were first properly normalised and the background levels subtracted. Next, multiexponential curve fits of the decay curves were performed using the computer code DISCRETE [25]. The lifetimes obtained from this analysis are presented in Table I. Notice here that all of the decays are represented by one or two exponentials, which is in contrast to the analysis of O IV and F V. The multiexponential fits provided good analytical descriptions of the data, which were used in cascade analyses using the computer code CANDY [16]. However, the raw normalised data were also used in the ANDC analysis, using the original formulation of the method by Curtis *et al.* [7] as a check. The data were also tested utilizing the CANYL code [26].

All data sets were carefully checked for the position of the "time zero" of excitation at the foil, which was located by observing the rapid rise at the early part of the measured decay. This is used to place the primary and cascade decay curves on a common time scale that is needed to perform a proper cascade correction. The decay curves can be shifted by a small amount due to, *e.g.*, bulging foils (as described in Ref. [27]).

Table I. *Multiexponential decomposition of the measured decay curves*

Transitions	N^a	τ^b/ns
2s2p3d ^{4}F–2s2p4f ^{4}G	5	0.61 ± 0.18 (3.6 ± 0.6)
2s2p3p ^{4}D–2s2p4d ^{4}F	5	1.3 ± 0.3 (6.4 ± 0.8)
2s2p3s $^4P_{1/2}$–2s2p4p $^4D_{3/2,\,1/2}$	4	0.45 ± 0.20^c
2s2p3s $^4P_{5/2,\,3/2}$–2s2p4p $^4D_{7/2,\,5/2}$	4	2.7 ± 0.8^c
2s2p3p $^4D_{7/2}$–2s2p3d $^4F_{9/2}$	4	14.6 ± 0.6 (−2.4 ± 0.7)
2s2p3p $^4D_{5/2}$–2s2p3d $^4F_{7/2}$	4	13.1 ± 1.2 (−4.5 ± 1.0)
2s2p3p $^4D_{3/2,\,1/2}$–2s2p3d $^4F_{5/2,\,3/2}$	4	13.6 ± 1.5 (−1.8 ± 1.1)
2s2p3s $^4P_{5/2}$–2s2p3p $^4D_{7/2}$	4	16.7 ± 0.6 (−8.3 ± 0.6)
2s2p3s $^4P_{5/2}$–2s2p3p $^4D_{5/2}$	4	14.8 ± 0.7 (−10.9 ± 0.8)
2s2p3s $^4P_{3/2}$–2s2p3p $^4D_{3/2}$	4	14.3 ± 1.0 (−10.0 ± 1.0)
2s2p3s $^4P_{3/2,\,1/2}$–2s2p3p $^4D_{5/2,\,3/2}$	4	14.3 ± 0.6 (−12.8 ± 0.6)
2s2p3s $^4P_{5/2}$–2s2p3p $^4P_{5/2}$	4	5.1 ± 0.2
2s2p3s $^4P_{5/2}$–2s2p3p $^4P_{3/2}$	4	5.4 ± 0.2
2s2p3s $^4P_{5/2}$–2s2p3p $^4S_{3/2}$	4	8.8 ± 0.5
2p^3 $^4S_{3/2}$–2p^{2}3d ^{4}P	4	2.3 ± 0.1
2p^3 $^4S_{3/2}$–2p^{2}3s ^{4}P	4	3.0 ± 0.1
2s2p^2 ^{4}P–2p^3 $^4S_{3/2}$	4	0.31 ± 0.05 (0.12 ± 0.04)
2s2p^2 $^2D_{5/2}$–2s^{2}3p $^2P_{3/2}$	4	1.7 ± 0.1
2s2p^2 $^2D_{3/2}$–2s^{2}3p $^2P_{1/2}$	4	4.1 ± 0.2
2s2p^2 ^{2}D–2p^3 ^{2}D	4	0.64 ± 0.05
2s2p^2 ^{2}D–2p^3 ^{2}P	4	0.28 ± 0.04
2s^{2}2p $^2P_{3/2}$–2s2p^2 $^2P_{3/2}$	6	0.22 ± 0.06
2s^{2}2p $^2P_{1/2}$–2s2p^2 $^2P_{1/2}$	5	0.19 ± 0.05
2s^{2}2p $^2P_{3/2}$–2s2p^2 $^2S_{1/2}$	4	0.32 ± 0.06 (1.5 ± 0.2)
2s^{2}2p $^2P_{3/2}$–2s2p^2 $^2D_{5/2}$	4	2.1 ± 0.1
2s^{2}2p $^2P_{1/2}$–2s2p^2 $^2D_{3/2}$	4	2.1 ± 0.1

[a] Number of analyzed decay curves.
[b] First entry refers to the primary lifetime whereas cascade components are given in parentheses. A negative sign indicates that this exponential has a negative amplitude.
[c] Measured in one unresolved line.

The lifetimes of the 3p ^{4}D and the 3d ^{4}F levels are all within 25% of each other in magnitude and affected by cascade repopulation, and a multiexponential decomposition is an unreliable method for their extraction. The first 45 ns of the decay curves of all the 3d ^{4}F levels exhibit a growing-in behaviour (see Fig. 3) and the inclusion in the ANDC analysis of the cascades from the 4f ^{4}G levels do not account for this behaviour. An inversion of the ANDC analysis [28] indicates the influence of a cascade decay curve (of unspecified origin) with a lifetime of approximately 3 ns. The only other configuration in the $n = 4$ complex that could repopulate the 3d ^{4}F is the 4p, and calculations for the 4p ^{4}D predict lifetimes of about 3 ns for $J = \frac{7}{2}$ and $\frac{5}{2}$ and of about 1 ns for $J = \frac{3}{2}$ and $\frac{1}{2}$. The only means available to measure the decay of these levels was via the unresolved blend containing the 3s ^{4}P–4p ^{4}D line at 1120 Å. Measurements of this decay curve reproducibly yielded two exponential components of lifetimes 0.45 ns and 2.7 ns. In the cascade analysis we used the 2.7 ns component to represent $J = \frac{7}{2}$ and $J = \frac{5}{2}$ in the 4p ^{4}D term and the 0.45 ns component to represent $J = \frac{3}{2}$ and $J = \frac{1}{2}$. The possible cascades from 2p^{2}3d ^{4}F were also considered, but the line was found to be weak. The second complication for the measurements of 3d $^4F_{7/2}$ and 3d $^4F_{5/2}$ is the blend by N II 3p $^3D_1$–3d $^1D_2$ [29]. To study that influence, the decay behaviour of the 3d ^{1}D was measured by studying the 3p $^1P_1$–3d $^1D_2$ line at 4448.28 Å. It has a rapid decay compared to the 2s2p3p and 3d quartet levels, which was not apparent in the decay curves measured at 4860, 4862.6 and 4868.5 Å. The assumption was made that the influence is negligible. We were forced to measure the 3d $^4F_{5/2}$ and 3d $^4F_{3/2}$ components in the unresolved line blend at 4860 Å. The decays of $^4F_{7/2}$ and $^4F_{9/2}$ were measured at 4862.6 and 4868.5 Å respectively.

To discuss the analysis of the 3p ^{4}D levels, we again refer to Fig. 1. To determine the lifetime of the 3p $^4D_{7/2}$ level, the primary decay curve was measured in the 4516.14 Å branch to 3s $^4P_{5/2}$. Incorporated into its cascade analysis were the decay curve from 4d ^{4}F as an unresolved multiplet, and the decay curves from 3d $^4F_{7/2}$ and 3d $^4F_{9/2}$. In contrast to the analysis in O IV and F V [3, 26], the curve fitting did not

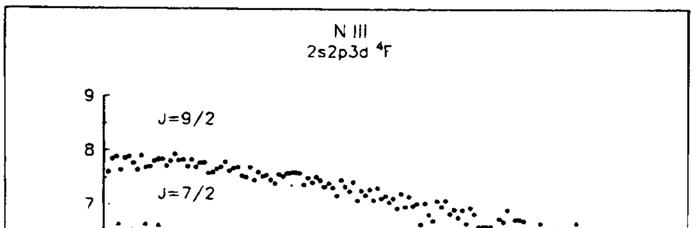

Fig. 3. Semilogarithmic plot of the measured decay curves for the fine structure levels in 2s2p3d ^{4}F in N III. The curves are drawn in the same scale but shifted vertically.

Table II. *Final experimental and theoretical lifetimes*

Level	τ_{exp} [a]	τ_{exp} [b]	τ_{th} [c]	τ_{th} [d]
$2s2p3d\,^4F_{9/2}$	12.7 ± 0.6	16.3 ± 0.16	16.2	11.6
$2s2p3d\,^4F_{7/2}$	10.5 ± 1.2	16.1 ± 0.17 [e]	14.1	9.4
$2s2p3p\,^4D_{7/2}$	13.0 ± 0.7	12.7 ± 0.9	14.6	15.2
$2s2p3p\,^4D_{5/2}$	11.4 ± 0.9	12.7 ± 0.9	14.7	15.2
$2s2p3p\,^4D_{3/2}$	11.7 ± 1.0	12.8 ± 0.9	11.7	14.1
$2p^3\,^4S_{3/2}$	0.26 ± 0.05		0.20	
$2s2p^2\,^2P_{3/2}$	0.20 ± 0.06		0.17	
$2s2p^2\,^2P_{1/2}$	0.19 ± 0.05		0.17	
$2s2p^2\,^2S_{1/2}$	0.32 ± 0.06		0.36	
$2s2p^2\,^2D_{5/2}$	2.09 ± 0.08		1.97	
$2s2p^2\,^2D_{3/2}$	2.09 ± 0.08		1.97	

[a] Results from ANDC analyses.
[b] Results from [2]. The values for the $3d\,^4F$ levels are from curve fits.
[c] Theoretical values from [6, 19].
[d] Theoretical values from [4].
[e] Average of two values in [2].

give any negative amplitude for the primary component. The next level is the $3p\,^4D_{5/2}$, for which we specified the primary decay curve by using the $\frac{5}{2}$–$\frac{7}{2}$ line at 4535.85 Å. For cascades we used decay curves of the $4d\,^4F$, the $3d\,^4F_{7/2}$ and the unresolved measurement of $^4F_{5/2}$ and $^4F_{3/2}$. It was not possible to do a cascade correction using the $\frac{5}{2}$–$\frac{5}{2}$ component at 4874.96 Å, because of the weakness of that line. Similarly we analyzed the $3p\,^4D_{3/2}$ by looking at the $\frac{3}{2}$–$\frac{3}{2}$ component at 4524.85 Å. As mentioned in the previous section, the $^4D_{1/2}$ level could not be measured since the $\frac{1}{2}$–$\frac{1}{2}$ transition at 4519.32 Å was too weak. That level could not be measured in O IV either, but in this case it was because of a blend by an O II line. Finally we also measured the $3p\,^4P_{5/2}$, the $3p\,^4P_{3/2}$ and the $3p\,^4S_{3/2}$ levels for completeness and included them in Table I. The $3p\,^4P$ lifetimes agree with the cascade-corrected values reported in [9]. For the $3p\,^4S_{3/2}$ the lifetime measurement agrees with [10] while the value reported in [15] was shorter.

Turning to the analysis of the $2s2p^2$ and $2p^3$ levels, we again refer to Fig. 2. The cascade correction made only small changes of the lifetimes for these levels. The largest change was for the $2p^3\,^4S_{3/2}$ level where the extracted lifetime decreased from 0.31 to 0.26 ns. Similarly, for $2s2p^2\,^2P_{3/2}$ the extracted lifetime decreased from 0.22 to 0.20 ns. That is, however, within the statistical error bars. The final result for the N III levels are presented in Table II.

4. Discussion

We have observed a pronounced J-dependence in the lifetimes of the $3d\,^4F$ levels in N III, similar to those reported earlier for F V [1] and O IV [3]. Theoretical explanations for these effects have been given in [1, 3] and involve the opening of additional decay channels to certain levels as a result of two types of intermediate coupling. One concerns the mixing between $3p\,^4D$ and $3p\,^2P$ levels, which opens additional decay channels to the $2s^22p\,^2P$ ground term. Another involves mixing between levels of the $3d\,^4F$ and $3d\,^4D$ terms, which provides the $^4F_{3/2}$, $^4F_{5/2}$ and $^4F_{7/2}$ levels with extra decay channels to the $2s2p^2\,^4P$ levels. The remaining 3d levels in the ^4P and ^4D terms have direct channels to $2s2p^2\,^4P$ and thus have short lifetimes and are weak or absent in the spectrum. Thus, for those levels with extra channels the lifetimes are reduced.

As can be seen from Table II the qualitative agreement between experiment and theory for $3d\,^4F$ is good and a J-dependence is noticed. The $^4F_{9/2}$ level has a lifetime that is approximately 2 ns longer than the other ^4F levels. For the $3p\,^4D_{7/2}$ and $^4D_{5/2}$ levels we measure a small difference that is not predicted by theory. However the error bars overlap, so no difference can be claimed on the basis of these experiment, which was also shown in [2]. We also notice good agreement for $4f\,^4G$, $4d\,^4F$ and $3p\,^4S_{3/2}$, where a theoretical calculation similar to the one in [4] yields 0.68, 1.70 and 8.72 ns respectively. For $3p\,^4P_{5/2}$ and $^4P_{3/2}$ however, theory gives lifetimes that are 4.26 and 4.27 ns, which is about 1 ns shorter than experiment.

In Figs 4 and 5 the isoelectronic comparison between theory and experimental data is shown. The experimental points for F V and O IV are taken from Refs [1] and [3] and the N III points are the work reported here. The theoretical lifetimes represented by dots connected with lines are from Ref. [6], while the triangles are superposition-of-configuration calculations Ref. [4]. The latter gives qualitatively better agreement with the trend in the sequence for $3d\,^4F_{9/2}$,

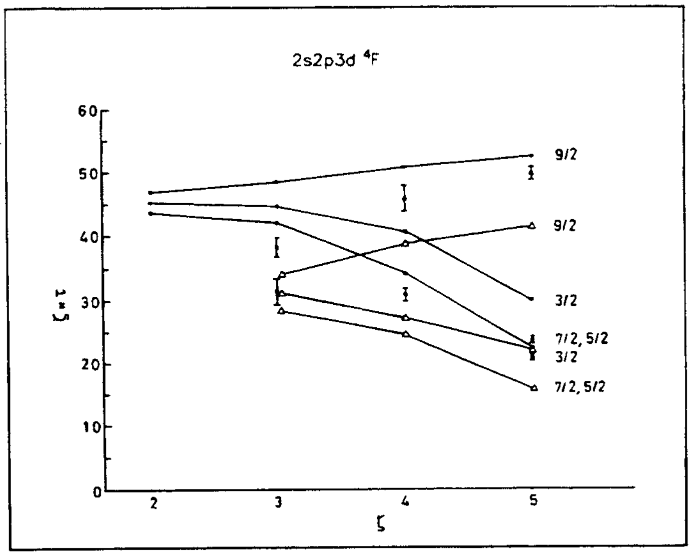

Fig. 4. Isoelectronic behaviour of the lifetimes of the $2s2p3d\,^4F$ terms. The dots connected with lines represent the theoretical values from [6] and the triangles represent the values from [4].

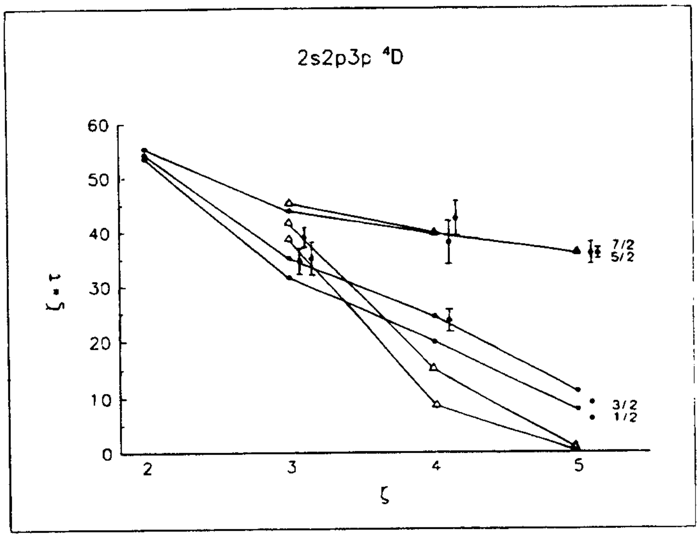

Fig. 5. Isoelectronic behaviour of the lifetimes of the $2s2p3p\,^4D$ term. The dots connected with lines represent the theoretical values from Ref. [6] and the triangles are the values from Ref. [4].

whereas the former gives a generally better description for the 3p ^{4}D levels (Fig. 5).

This investigation has shown that, except for the 2s2p3d ^{4}F levels, there is good agreement between the available calculations in the sequence and the observed lifetime data. For the 3d ^{4}F levels a systematic discrepancy exists, whereby the differences among the lifetimes agree with theory but the absolute values do not. While agreement is good for F V, the calculated values for the lifetimes in O IV and N III become increasingly longer than the measured values. It is hoped that this will encourage further calculations.

Acknowledgements

We are grateful to G. Miecznik, T. Brage and C. Froese Fischer for the use of their theoretical data prior to publication. The work was partially supported by the U.S. Department of Energy, Fundamental Interactions Branch, Office of Basic Energy Sciences, Division of Chemical Sciences, under Grant Number DE-FG02-94ER14461.

References

1. Engström, L., Reistad, N. and Westerlind, M., Physica Scripta **44**, 548 (1991).
2. Kotzé, T. C., van der Westhuizein, P. and Visser, K., Phys. Rev. **A44**, 4180 (1991).
3. Westerlind, M., Bengtsson, P., Kirm, M. and Engström, L., J. Phys. B: At. Mol. Opt. Phys. **27**, 877 (1994).
4. Westerlind, M., Thesis, University of Lund (1992).
5. Cowan, R. D., "The Theory of Atomic Structure and Spectra" (Univ. of California Press, Berkeley 1981).
6. Miecznik, G., Brage, T. and Froese Fischer, C., J. Phys. B: At. Mol. Opt. Phys. (in press).
7. Curtis, L. J., Berry, H. G. and Bromander, J., Phys. Lett. **A34**, 169 (1971).
8. Curtis, L. J., "Lifetime Measurements", in: "Beam-Foil Spectroscopy" (Edited by S. Bashkin) (Springer, Berlin 1976) pp. 63–109.
9. van der Westhuizen, P., Coetzer, F. J. and Kotzé, T. C. "Atomic Spectra and Oscillator Strengths for Astrophysics and Fusion Research" (Edited by J. E. Hansen) (North Holland Publ., Amsterdam 1990) pp. 182–3.
10. Pinnington, E. H., Nucl. Instr. Meth. **90**, 93 (1970).
11. Denis, A., Désesquelles, J., Dufay, M. and Poulizac, M. C., C.R. Acad. Sc. Paris **266**, 64 (1968).
12. Ceyzeriat, P., Denis, A., Désesquelles, J., Druetta, M. and Poulizac, M. C., Nucl. Instr. Meth. **90**, 103 (1970).
13. Fink, U., McIntyre, G. N. and Bashkin, S., J. Opt. Soc. Am. **58**, 475 (1968).
14. Pinnington, E. H. and Lin, C.-C., J. Opt. Soc. Am. **59**, 717 (1969).
15. Brink, J. A. *et al.*, Z. Physik **A288**, 1 (1978).
16. Engström, L., Nucl. Instr. Meth. **202**, 369 (1982).
17. Stafford, R. P., Hibbert, A. and Bell, K. L., Mon. Not. R. Astron. Soc. **260**, L11 (1993).
18. Fang, Z., Kwong, V. H. S. and Parkinson, W. H., Astrophys. J. **413**, L141 (1993).
19. Brage, T. *et al.* (to be published).
20. Reistad, N., Hutton, R., Nilsson, A. E. and Martinson, I., Physica Scripta **34**, 151 (1986).
21. Haar, R. R. *et al.*, Nucl. Instr. Meth. Phys. Res. **B79**, 746 (1993).
22. Haar, R. R. and Curtis, L. J., Nucl. Instr. Meth. Phys. Res. **B79**, 782 (1993).
23. Michels, D. J., J. Opt. Soc. Am. **64**, 1164 (1974).
24. Striganov, A. R. and Svetitskii, N. J., "Tables of Spectral lines of Neutral and Ionized Atoms" (Plenum, New York 1968).
25. Provencher, S. W., J. Chem. Phys. **64**, 2772 (1976).
26. Engström, L., J. Phys. B: At. Mol. Opt. Phys. **24**, 5077 (1991).
27. Engström, L. and Bengtsson, P., Physica Scripta **43**, 480 (1991).
28. Kohl, J. L., Curtis, L. J., Schectman, R. M. and Chojnacki, D. A., J. Opt. Soc. Am. **61**, 1656 (1971).
29. Eriksson, K. B., Ark. Fysik **13**, 303 (1958).